

COMPUTATION OF WAKEFIELDS FOR AN IN-VACUUM UNDULATOR AT PETRA III

E. Gjonaj*, L. Lünzer, T. Weiland, Technische Universität Darmstadt, TEMF, Darmstadt, Germany
R. Wanzenberg, DESY, Hamburg, Germany

Abstract

At DESY the installation of an in-vacuum undulator at the synchrotron radiation facility PETRA III is under consideration. The movable magnet array of the undulator is installed inside the vacuum chamber to achieve shorter wavelength synchrotron radiation. A thin metal foil covers the magnet structure to mitigate resistive wall wakefields. Movable tapered transitions connect the magnet structure and the adjacent vacuum duct to reduce geometric wakefields. Nevertheless these movable tapered transitions contribute significantly to the impedance budget of PETRA III. The computer codes MAFIA, CST-Studio and PBCI have been used to calculate the longitudinal wakefields. We perform an investigation on the accuracy of these codes for this very smoothly tapered geometry. The results for the loss parameters of the movable transitions for different undulator gap widths are presented.

INTRODUCTION

Since the end of 2012 all 14 beam lines of the synchrotron light source PETRA III at DESY [1] are available for users. The commissioning of the light source started in 2009 and user operation started in summer 2010 [2]. The very low horizontal emittance of 1 nm rad has been achieved with the help of 20 damping wigglers with a length of 4 m each [3]. PETRA III was initially running with positrons since PETRA shared the preaccelerator chain with the light source DORIS, which was running with positrons to avoid problems with ionized dust particles. DORIS was shut down at the end of 2012, and PETRA III is operated with electrons since January 2013. The insertion devices are installed in one octant of the PETRA III ring. A double bend achromat (DBA) lattice with eight straight sections provides in each section space for a 5 m long, or two 2 m long insertion devices which a separation angle of 5 μ rad which is obtain with a short dipole magnet between the insertion devices. Presently six different types of insertion devices are installed at PETRA III, see [4, 5]. The minimum magnetic gap of the planar undulators is 9.5 mm and the inner vertical aperture of the vacuum chamber in the undulator is 7 mm. It is now considered to replace one of the 5 m long undulators (type U29 [4]) with an in-vacuum undulator (IVU) for the hard X-ray material science beam line. More than 20 IVUs are installed in

Spring-8 [6] and have been proved to be a promising way toward shorter wavelength of synchrotron radiation.

An impedance model of PETRA III was developed in collaboration with DESY, the University of Darmstadt, the Otto-von-Guericke University of Magdeburg, CANDLE (Yerevan, Armenia) and the Budker Institute BINP (Novosibirsk, Russia), see [7]. At the entrance and at the exit of each straight section a tapered transition (length 115 mm) is installed to reduce the impedance of PETRA III [8]. In the following, numerically computed loss ($k_{||}$) and kick parameters (k_{\perp}), respectively, have been used to characterize the impedance of these components in the ring.

WAKE COMPUTATIONS

There are mainly two contribution to the impedance from the IVU: the resistive wall contribution from the magnetic material and the geometric wakefield from the tapered transitions. The magnetic poles are covered with a Cu-Ni sheet to mitigate the resistive wall contribution, see also [6]. In this paper the contribution to the geometric wake field is calculated using numerical codes. The wakefield solver of the MAFIA and CST group of codes [9] and the Parallel Beam Cavity Interaction (PBCI) [10] code were used to calculate the wake potential for a Gaussian bunch ($\sigma_z = 10$ mm).

A schematic presentation of the tapered transitions in front of the 4 m long IVU is shown in Fig. 1. The first tapered transition is the the “standard” transition which is installed at the entrance and exit of all eight straight sections in the new octant of PETRA III. The loss and kick parameters of this transition are reported in Ref. [8]. For the vacuum design of the IVU-section it was decided to keep the “standard” transition in place and to add an additional movable tapered transition which smoothly follows the gap movement of the IVU. There is an additional transition (95 mm long) in front of the vacuum tank of the IVU which connects the small gap chamber in front of the IVU to the IVU vacuum tank (diameter 250 mm).

The movable transitions and a shortened (1/10) version of the vacuum tank have been modeled for the wake field calculated with MAFIA, see Fig. 2 using a mesh with a step size of 1 mm. The results for the calculations are summarized in Table 1.

* gjonaj@temf.tu-darmstadt.de

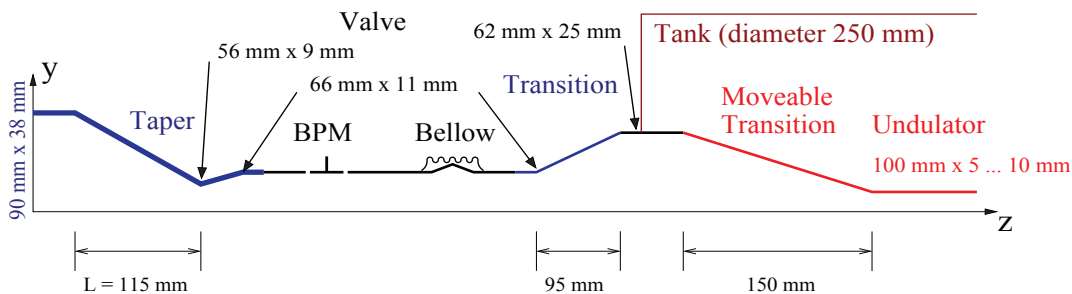


Figure 1: Schematic presentation of the tapered transition in front of the in-vacuum undulator.

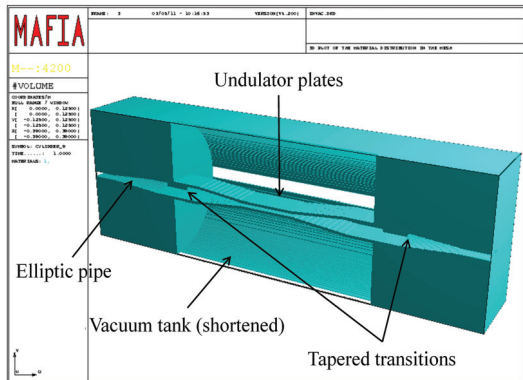


Figure 2: Model of the IVU tank with two movable transitions for the MAFIA calculations. In the model the vacuum tank is assumed to be only 0.4 m long. The tapers have the correct lengths. An undulator gap of 6 mm is considered.

Table 1: Loss and kick parameter for one tapered transition

| | $k_{ } / V/nV$ | $k_{\perp} / V/(pC m)$ |
|---------------------------------|-----------------|------------------------|
| Results from Ref. [8, 7] | | |
| “standard” transition | -5.2 | 62.8 |
| Bellow | -13.7 | 14.9 |
| BPM | -0.16 | 3.87 |
| Movable transitions | | |
| MAFIA (1 mm mesh) | -5.5 | - |

CST PS AND PBCI SIMULATIONS

In order to achieve possibly more accurate results, two more codes, CST PS™ and PBCI have been used in the simulation of the full IVU geometry including both movable transitions. These codes offer a number of advanced capabilities for wakefield calculations such as dispersion-free algorithms, Perfect Boundary Approximation (PBA), moving window and parallelization. A summary of these features is given in Table 2 (cf. also [10]).

Figure 3 shows a comparison of the longitudinal wake potentials for one tapered transition computed with each of the three codes when a ‘standard’ discretization with 10 mesh points per bunch length is applied. Large discrepan-

Table 2: Features of the Codes Used in the Calculations

| Feature/Code | PBCI | CST PS | MAFIA |
|-----------------|-----------|---------|------------|
| Dispersion-free | yes | no | no |
| Moving window | yes | no | no |
| Boundaries | staircase | PBA | staircase+ |
| Parallelization | MPI | MPI/GPU | none |

cies are observed, in particular, between the CST PS on the one hand and PBCI and MAFIA on the other. This behavior is due to the low accuracy of EM solvers for slowly tapered structures; an observation which has been previously made by several authors (cf. [11] and references therein).

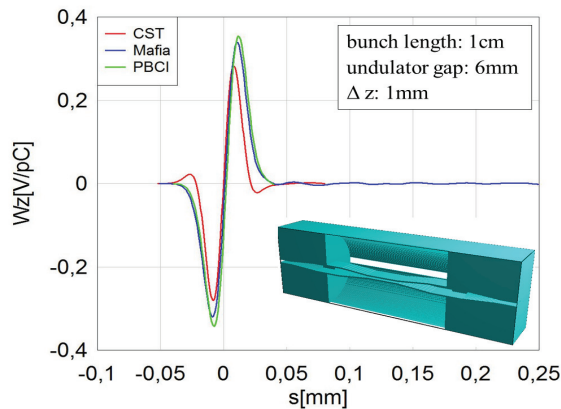


Figure 3: Longitudinal wake potentials computed with a standard mesh with 10 points / bunch length.

The difficulty in the numerical simulation of the IVU structure is illustrated in Fig. 4 and Fig. 5 for the case of a fixed gap width of 6mm. Obviously, in PBCI a discretization with up to 1280 mesh points per bunch length in the longitudinal direction is necessary to obtain an estimated error below 1%. A numerical simulation at this resolution is only possible because of the use of the moving window approach. Also, an anisotropic mesh is applied which is much sparser in the transverse direction along the broader side of the tapered structure. Nevertheless, the model at finest resolution contains more than 200 million mesh cells which results in a computational time of 56 hours in a 2040

node cluster. As can be seen in Fig. 4 the convergence rate is reduced to first order which is attributed to the less accurate staircase approximation employed by this code.

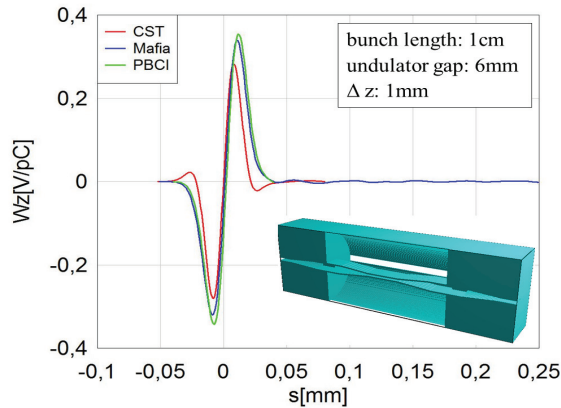


Figure 4: Numerical error and convergence rate of PBCI for different mesh resolutions in the 6mm gap case.

A better numerical behavior is observed in CST PS simulations (see Fig. 5). The 2nd order convergence is recovered due to the better approximation of geometry. Thus, a much sparser mesh than in PBCI is needed for the same accuracy. However, due to the global window approach used in CST PS, the best accuracy at the finest possible mesh resolution as well as the total computational times are quite comparable to those of PBCI.

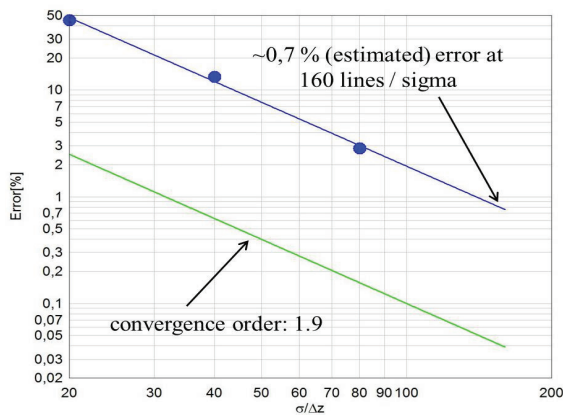


Figure 5: Numerical error and convergence rate of CST PS for different mesh resolutions in the 6mm gap case.

The loss parameters obtained by the two codes in the 6mm gap case are shown in Fig. 6. Remarkably, CST PS and PBCI converge from opposite directions. A more accurate estimation for the final value of the loss parameter can, thus, be obtained by averaging the results of the two codes at the respective finest mesh resolution. Also note that the loss parameters displayed in Fig. 6 are not comparable to the MAFIA result (Table 1) since the latter was obtained for a single tapered transition only. The simulation results for different gap widths are summarized in (Table 3).

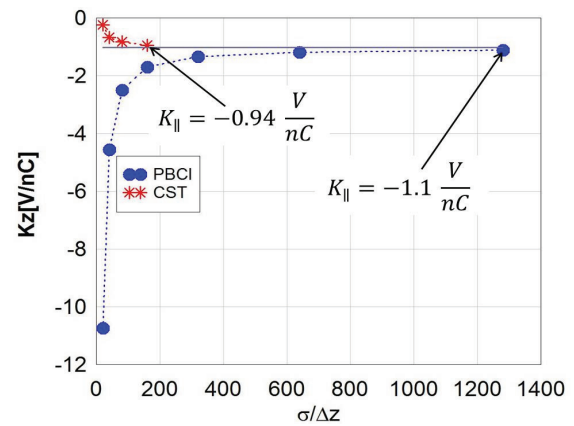


Figure 6: Numerical error and convergence rate of CST PS for different mesh resolutions in the 6mm gap case.

Table 3: Loss parameters (V/nC) of the tapered IVU transitions computed for different gap widths

| Code/Gap | 5mm | 6mm | 7mm | 10mm |
|----------|-------|-------|-------|-------|
| CST PS | -0.95 | -0.94 | -0.85 | -0.72 |
| PBCI | -1.15 | -1.10 | -1.02 | -0.84 |

CONCLUSION

The loss parameters of the movable tapered transitions of PETRA III have been calculated for different widths using different codes. With CST PS and PBCI it is possible to perform full scale simulations including both transitions and the vacuum tank of the IVU. It was noted, however, that these simulations are extremely costly due to the low numerical accuracy for this slowly tapered geometry. At the finest mesh resolution the results obtained from both codes are in very good agreement with an estimated error of less than 1% for the longitudinal wake potential.

ACKNOWLEDGMENTS

The authors thank DESY for supporting this work.

REFERENCES

- [1] K. Balewski et al. (eds.), DESY 2004-035.
- [2] K. Balewski, IPAC'10, TUXRA01.
- [3] M. Tischer et al., EPAC'08, WEPC132.
- [4] M. Tischer et al., AIP Conf. Proc. **879** (2007) 343.
- [5] M. Tischer et al., EPAC'08, WEPC133.
- [6] T. Tanaka et al., FEL'05, TUOC001.
- [7] W. Chou, R. Wanzenberg (eds.), ICFA Beam Dynamics Newsletter **45**, April 2008.
- [8] K. Balewski et al., PAC'05, FRPMN018.
- [9] "MAFIA 4" and "CST PS", CST AG, Darmstadt, Germany.
- [10] E. Gjonaj et al., ICAP'06, MOM2IS02.
- [11] B. Podobedov, IPAC'12, WEP100.